

Article

An Alternative Approach for Identifying Nonlinear Dynamics of the Cascade Logistic-Cubic System

Yanan Liao ^{1,2}, Kai Yang ^{1,2}, Hua Wang ^{1,2} and Qingtai Xiao ^{1,2,*} 

¹ State Key Laboratory of Complex Nonferrous Metal Resources Clean Utilization, Kunming University of Science and Technology, Kunming 650093, China; liaoyanan6@163.com (Y.L.); kaiyang@stu.kust.edu.cn (K.Y.); wanghua@kust.edu.cn (H.W.)

² Faculty of Metallurgical and Energy Engineering, Kunming University of Science and Technology, Kunming 650093, China

* Correspondence: qingtai.xiao@kust.edu.cn

Abstract: The 0-1 test for chaos, which is a simple binary method, has been widely used to detect the nonlinear behaviors of the non-cascade chaotic dynamics. In this paper, the validity checks of the 0-1 test for chaos to the popular cascade Logistic-Cubic (L-C) system is conducted through exploring the effects of sensitivity parameters. Results show that the periodic, weak-chaotic, and strong-chaotic states of the cascade L-C system can be effectively identified by the introduced simple method for detecting chaos. Nevertheless, the two sensitivity parameters, including the frequency ω and the amplitude α , are critical for the chaos indicator (i.e., the median of asymptotic growth rate, K_m) when the cascade dynamic is detected by the method. It is found that the effect of α is more sensitive than that of ω on K_m regarding the three dynamical states of the cascade L-C system. Meanwhile, it is recommended that the three states are identified according to the change of K with α from zero to ten since the periodic and weak-chaotic states cannot be identified when the α is greater than a certain constant. In addition, the modified mean square displacement $D_c^*(n)$ fails to distinguish its periodic and weak-chaotic states, whereas it can obviously distinguish the above two and strong-chaotic states. This work is therefore invaluable to gaining insight into the understanding of the complex nonlinearity of other different cascade dynamical systems with indicator comparison.

Keywords: 0-1 test for chaos; sensitivity parameter; cascade dynamic system; Logistic-Cubic mapping; noised time series analysis

MSC: 37N30



Citation: Liao, Y.; Yang, K.; Wang, H.; Xiao, Q. An Alternative Approach for Identifying Nonlinear Dynamics of the Cascade Logistic-Cubic System. *Mathematics* **2022**, *10*, 2080. <https://doi.org/10.3390/math10122080>

Academic Editors: Min Wang, Haijun Gong, Liucang Wu and Songfeng Zheng

Received: 18 April 2022

Accepted: 14 June 2022

Published: 15 June 2022

Publisher's Note: MDPI stays neutral with regard to jurisdictional claims in published maps and institutional affiliations.



Copyright: © 2022 by the authors. Licensee MDPI, Basel, Switzerland. This article is an open access article distributed under the terms and conditions of the Creative Commons Attribution (CC BY) license (<https://creativecommons.org/licenses/by/4.0/>).

1. Introduction

Chaos has been widely used in biononlinear dynamics [1,2], encryption algorithm [3,4], physics [5,6], and industrial mixing [7,8]. The long-standing fundamental issue related to chaotic dynamics is the determination of regular, chaotic, or random for a nonlinear dynamic system. From open literature, a variety of methods, including power spectra, entropy, fractal dimension, and Lyapunov exponent, have been used to address it [9]. However, these methods own certain limitations. For example, the most popular method is to calculate the maximal Lyapunov exponent, but phase space reconstruction is complex and not inevitable for dynamic systems whose equations are unknown [10]. However, the 0-1 test for chaos works directly with the time series and does not require any phase space reconstruction. It has also been found in applications in a wide range of fields.

In particular, the 0-1 test for chaos can be applied to the chaotic detection of uncertain dynamical systems without fundamental equations. The input is time-series data, and the output is zero or one depending on whether the dynamics are non-chaotic or chaotic [10]. Currently, the 0-1 test for chaos has been widely used in many new fields, including nonlinear noise reduction [10–12], epidemic model [13,14], and communication

technology [15,16] due to its advantages such as simplicity of theoretical fundamental, convenience of implementation, and high-accuracy of chaos identification. In this regard, the theoretical background of the 0-1 test for chaos has already been reported, which should be highlighted. For instance, Gottwald and Melbourne (2009) deeply studied the improvement effect of the 0-1 test for chaos on the detection performance of noised signals [17]. Armand Eyebe Fouda et al. (2014) applied the binary 0-1 test for chaos to a discrete mapping of the local maxima and minima of the original observable object [18]. Muthu et al. (2020) used the 0-1 test for chaos and three state tests to classify the chaotic state of Logistic Tent system into strong-chaotic and weak-chaotic [19]. Xiao et al. (2022) discussed the influence of damping amplitude on chaos detection reliability of the modified 0-1 test for chaos for oversampled and noisy observations [20].

In addition, the cascade systems can improve the chaotic and onto-mapping parameter range while considering the high computation efficiency and be used to optimize the dynamic characteristics [21]. Compared with one-dimensional chaotic systems, the cascade chaotic systems own more complexity. Compared with the high-dimensional chaotic dynamics, the cascade chaotic systems are simpler and need a short time to generate discrete data sequence. Recently, the cascade chaotic system technology has also been widely used in image encryption, voice communication, and industrial mixing. For example, Zhuang et al. (2018) proposed an encryption algorithm based on improved Josephus loop and Logistic mapping for scrambling blocks [22], Guo (2020) constructed a new cascade Logistic-Fibonacci chaotic system to generate random sequences [23], and Cheng et al. (2021) proposed a novel image encryption scheme based on a hybrid cascaded chaotic system and sectoral segmentation [24]. These cascade chaotic algorithms greatly improve the sensitivity of high-dimensional and maintain the rapidity of low-dimensional chaotic systems and have been also widely used in the field of communication. For instance, Jin et al. (2009) cascaded multiple Logistic subsystems with different parameters to construct a Logistic-Logistic speech frequency domain real-time encryption system [25]. Yu et al. (2016) proposed a method of constructing the Logistic-Chebyshev chaotic mapping which is used to effectively expand the key space of the chaotic system [26]. Zhao (2021) proposed a spread spectrum code generation algorithm based on cascade Sine-Tent coupled chaotic mapping [27]. Meanwhile, the cascade chaotic system has also been applied in the field of industrial stirring. Zhang et al. (2021) proposed a Logistic cascade sequence to generate chaotic speed to improve the quality of the solid-liquid mixing state [28].

Inspired and motivated by the above text, it is of practical significance to investigate the characteristics of cascade chaotic systems by using 0-1 test for chaos. Furthermore, the validity of the 0-1 test for cascaded chaotic system is conducted in detail through exploring the effects of frequency parameter and amplitude parameter on the chaos indicator in this paper. It is worth noting that the availability of 0-1 test for chaos on the noisy cascaded chaotic dynamical system has also not yet been discussed. The 0-1 test for chaos would be a novel chaos detection method that can be directly applied to time series data generated by cascade system and does not require phase space reconstruction.

After Section 1, the paper is organized as follows. Initially, a brief description of the 0-1 test for chaos is presented and four different methods for obtaining the asymptotic growth rates are compared in Section 2. The approach to construct the cascade chaos formula of the Logistic-Cubic mapping and to generate the time series data for numerical experiments is then illustrated in Section 3. Afterwards, the results of numerical experiments regarding the effects of frequency, amplitude, and mean square displacement on the chaos indicator are analyzed in Section 4. Concluding remarks are then discussed.

2. 0-1 Test for Chaos

2.1. Traditional 0-1 Test for Chaos

The 0-1 test for chaos has been proposed to improve the convenience of chaos identification, and its test output do not rely on explicit equations. In a word, the input of the 0-1 test for chaos is a measured time series, and whether the dynamical system is chaotic or

not can be well distinguished by whether the output is 0 or 1. For the cascade dynamical system, the specific implementation steps of the 0-1 test for chaos are as follows. Firstly, let a discrete time series $x = (x_1, x_2, \dots, x_N)$, which can be interpreted as a vector containing N measured data points, be input. For random number $c \in (0, \pi)$, the translation variables are computed by

$$p_c(n) = \sum_{t=1}^n x_t \cos(tc) \tag{1}$$

and

$$q_c(n) = \sum_{t=1}^n x_t \sin(tc) \tag{2}$$

where $n = 1, 2, \dots, N$. The theory underlying the test ensures that if the underlying dynamical system is regular, the variables $p_c(n)$ and $q_c(n)$ exhibit a bounded evolution. On the other hand, if the system is chaotic, these variables exhibit asymptotically unbounded growth with features reminiscent of Brownian motion. Secondly, a modified mean square displacement (MSD) of $p_c(n)$ and $q_c(n)$ is calculated by

$$D_c(n) = M_c(n) - V_{\text{osc}}(c, n) \triangleq M_c(n) - (E(x))^2 \frac{1 - \cos(nc)}{1 - \cos c} \tag{3}$$

where $V_{\text{osc}}(c, n)$ refers to the oscillatory term and the mean square displacement $M_c(n)$ is given by

$$M_c(n) = \lim_{N \rightarrow \infty} \frac{1}{N} \sum_{t=1}^n \{ [p_c(t+n) - p_c(t)]^2 + [q_c(t+n) - q_c(t)]^2 \} \tag{4}$$

and the expectation $E(x)$ is given by

$$E(x) = \lim_{N \rightarrow \infty} \frac{1}{N} \sum_{t=1}^n x_t \tag{5}$$

where $D_c(n)$, which exhibits the same asymptotic growth as $M_c(n)$ but with better convergence properties, is the second indicator used to judge the chaotic characteristics in the underlying dynamical system. In other words, $D_c(n)$ is a bounded function in time if the given time series is regular, whereas $D_c(n)$ grows linearly with n if the given time series is chaotic. It should be noted that $n \ll N$ and the numerical value n is considered according to $n \leq n_{\text{cut}} = N/10$ in general. Thirdly, the asymptotic growth rate (AGR) K , which is the third indicator of the 0-1 test for chaos, is estimated quantificationally. In fact, there are two different methods, including regression and correlation for calculating AGR with original or modified MSD. There are hence various approaches for estimating AGR, and the different types of AGR are described below.

Here, four versions of AGR, including $K_{c1}(c)$, $K_{c2}(c)$, $K_{c3}(c)$, and $K_{c4}(c)$, are provided, as shown in Table 1. (1) The regression method is related to linear regression with the log-log plot. In terms of the original mean square displacement $M_c(n)$, the first version K_{c1} of K is given by

$$K_{c1}(c) = \lim_{N \rightarrow \infty} \frac{\log M_c(n)}{\log n} \tag{6}$$

where K_{c1} is numerically determined by fitting a straight line to the graph of $\log M_c(n)$ versus $\log n$ through minimizing the absolute deviation. (2) For demonstrating the effectiveness between the modified mean square displacement $D_c(n)$ and $M_c(n)$, the second version K_{c2} of K obtained using the regression method is given by

$$K_{c2}(c) = \lim_{N \rightarrow \infty} \frac{\log D_c(n)}{\log n} \tag{7}$$

where K_{c2} is numerically determined by fitting a straight line to the graph of $\log D_c(n)$

versus $\log n$ through minimizing the absolute deviation. (3) For demonstrating the effectiveness between the regression method and the correlation method, the third version K_{c3} of K obtained using the modified mean square displacement $D_c(n)$ is given by

$$K_{c3}(c) = \text{corr}(\xi, \Delta) = \frac{\text{cov}(\xi, \Delta)}{\sqrt{\text{var}(\xi)\text{var}(\Delta)}} \tag{8}$$

where $\text{cov}(\xi, \Delta)$, $\text{var}(\xi)$, and $\text{var}(\Delta)$ respectively indicate co-variance between n_{cut} -dimensional vectors $\xi = (1, 2, \dots, n_{\text{cut}})$ and $\Delta = (D_c(1), D_c(2), \dots, D_c(n_{\text{cut}}))$, variance of ξ , and variance of Δ . In practical terms, the correlation method has been proved to greatly outperform the regression method for different dynamical systems for public literature. In addition, the values of median K_m of K correspond to $K_{m1}(c)$, $K_{m2}(c)$, $K_{m3}(c)$, and $K_{m4}(c)$ and can be used to quantify the dynamical behaviors of the systems. In other words, $K_m \approx 0$ indicates regular dynamics, and $K_m \approx 1$ indicates chaotic dynamics.

Table 1. Various approaches for K estimation.

Version of K	Version of K_m	Estimation Method	Employed Approach
$K_{c1}(c)$	$K_{m1}(c)$	Regression	$M_c(n)$
$K_{c2}(c)$	$K_{m2}(c)$		$D_c(n)$
$K_{c3}(c)$	$K_{m3}(c)$	Correlation	$D_c(n)$
$K_{c4}(c)$	$K_{m4}(c)$		$D_c^*(n)$

2.2. Description of Issue Addressed

As mentioned in open literature, the original 0-1 test for chaos may be more efficient when the level of measurement noise is sufficiently small. In the real world, in fact, the measured time series data is mostly accompanied by noise with different types or levels. For making the 0-1 test for chaos more robust to the presence of measurement noise, the oscillatory term has been considered in the 0-1 test for chaos. Furthermore, to reduce the sensitivity of chaos detection to noise within the observed time series, the damped version of the 0-1 test for chaos is needed for identifying the cascade chaotic dynamics, and in this work the corresponding MSD is given by

$$D_c^*(n) = D_c(n) + \alpha V_{\text{damp}}(n) \triangleq D_c(n) + \alpha(E(x))^2 \sin(\omega n) \tag{9}$$

where $V_{\text{damp}}(n)$ refers to the damping term and the frequency parameter ω is chosen arbitrarily. The amplitude parameter α of the chaos indicator $D_c^*(n)$ controls the sensitivity of the test to weak noise and simultaneously to weak chaos within the observed time series generated by cascade chaotic dynamics. Therefore, the corresponding asymptotic growth rate K is also a chaos indicator for cascade chaotic dynamics and given by

$$K_{c4}(c) = \text{corr}(\xi, \Delta^*) = \frac{\text{cov}(\xi, \Delta^*)}{\sqrt{\text{var}(\xi) \cdot \text{var}(\Delta^*)}} \tag{10}$$

where $\Delta^* = (D_c^*(1), D_c^*(2), \dots, D_c^*(n_{\text{cut}}))$, $\text{cov}(\xi, \Delta^*)$ indicates co-variance of ξ and Δ^* , and $\text{var}(\Delta^*)$ indicates variance of Δ^* , respectively. Next, the noisy time series data originated from cascade chaotic dynamics is provided in the following section, after which the effects of sensitivity parameters, including damping amplitude parameter α and frequency parameter ω on different chaos indicators, are respectively discussed.

3. Description of the Synthetic Data

3.1. Dynamic Behaviors of Cascade System

Generally, Logistic mapping, which is used to generate time series data and owns well randomness, periodicity or chaoticity, is one of the most popular dynamical mappings with a simple mathematical form. In fact, Logistic mapping is defined as

$$x_{n+1} = \mu x_n(1 - x_n) \tag{11}$$

where the control parameter $\mu \in [0, 4]$ and $x_n, x_{n+1} \in [0, 1]$. The Logistic system is chaotic when $\mu \in [3.57, 4]$. Obviously, the range of the chaotic behavior is very limited, and this has limited the application of Logistic mapping. Therefore, it is essential to design new modified mathematical mappings with the improved chaotic behavior. In addition, Cubic mapping is another common dynamical mapping and is defined as

$$x_{n+1} = ax_n^3 - bx_n \tag{12}$$

where the control parameter $b \in [0, 3]$ and the mapping is when $b = 3$. In this work, $a = 0.5$. To obtain the cascade system combining Logistic and Cubic mappings, the cascade steps are provided below. Firstly, to construct the common mapping area of the Logistic and Cubic mappings, the original Cubic mapping is modified and given by

$$x_{n+1} = \left| \frac{x_n^3}{a^2} - bx_n \right| \tag{13}$$

where the control parameter $b \in [0, 3]$, $a = 0.5$, and $x \in [0, 2a]$, as mentioned above. The system is chaotic when $b \in [2.43, 3]$ and it is when $b = 3$. Then, the cascade chaotic system is given by

$$x_{n+1} = \left| 4\mu^3 x_n^3 (1 - x_n)^3 - 3\mu x_n (1 - x_n) \right| \tag{14}$$

where the control parameters $\mu \in [0, 4]$ and $x_n, x_{n+1} \in [0, 1]$. In order to reflect the improvement performance of the cascade system more intuitively, the chaotic characteristics of the above systems are compared, as shown in Table 2. As expected, the used cascade dynamical system in this work is obtained by combing Logistic mapping and the improved Cubic mapping. In addition, the cascade chaotic system (CCS) may own the extended onto mapping range of chaos, which is a better performance of CCS than that of Logistic mapping and the improved Cubic mapping. In fact, the advantage of CCS can enhance the chaotic characteristics and improve the chaotic key space. The generated chaotic sequences are subsequently tested by the chaos detection methods.

Table 2. Comparison of chaotic characteristics of Logistic, improved Cubic, and L-C mappings.

Type of Mapping	Control Parameters	Chaotic Interval	Interval of Onto Mapping
Logistic	$\mu \in [0, 4]$	$\mu \in [3.57, 4]$	$\mu = 4$
Improved Cubic	$b \in [0, 3]$	$b \in [0, 2a]$	$b = 3$
L-C	$\mu \in [0, 4]$	$\mu \in [1.55, 4]$	$\mu \in [1.9, 4]$

As shown in Figure 1a, the bifurcation diagram of the cascade L-C system for different numerical values of control parameter μ is present. In addition, Figure 1b presents the changing of K_{m3} for the cascade L-C system with $1 \leq \mu \leq 4$ increased in increments of 0.05. According to these two subfigures, it is meanwhile observed that the L-C system is chaotic in terms of the most range of $\mu \in [1.55, 4]$, and the asymptotic growth rate gradually approaches $K_{m3} = 1$ by increasing control parameter μ . The exhibited features in the former subfigure are in perfect agreement with that in the latter one. It is proved that the 0-1 test for chaos can identify the behaviors of the cascade L-C system. Due to the existence of the resonance phenomenon, the asymptotic growth rate drops suddenly from $K_{m3} = 1$ to $K_{m3} = 0$ in some periodic windows. Nonetheless, it is obvious that the cascade L-C system owns an expanded system parameter space, larger regions of chaotic states, and mapping ranges.

Figure 2 illustrates the graphical results of the 0-1 test for chaos for the cascade L-C system. There are three types of graphs, including translational variables ($p_n(n), q_c(n)$), the path of modified MSD ($n, D_c(n)$), and a single real number of AGR ($c, K_{m3}(c)$). According to this figure, the three subfigures in the top row show the results related to the periodic dynamic, the three subfigures in the medium row display the computations corresponding to the weak-chaotic dynamic with $K_{m3}(c) \in (0.5, 0.9]$, and the three sub-

figures in the bottom row illustrate the outputs in terms of the strong-chaotic dynamic with $K_{m3}(c) \in (0.9, 1]$. For periodic dynamic, the phase portrait $(p_c(n), q_c(n))$ exhibits a regular round, the plot of $(n, D_c(n))$ presents a nonlinear function, and the values of AGR are approaching $K_{m3}(c) = 0$ approximatively. For weak-chaotic dynamic, the phase portrait $(p_c(n), q_c(n))$ shows Brownian motion with low dispersion, the plot of $(n, D_c(n))$ presents a linear function with wide spanwise, and the values of AGR $K_{m3}(c)$ are tending to be normally distributed. For strong-chaotic dynamic, the phase portrait $(p_c(n), q_c(n))$ represents Brownian motion with great dispersion, the plot of $(n, D_c(n))$ presents a linear function with narrow spanwise, and the values of AGR are approaching $K_{m3}(c) = 1$ approximatively. Thus, the cascade L-C system has different dynamical states with different control parameter and deterministic chaos is verified. Compared to other methods, the 0-1 test for chaos has the advantage of not requiring the phase space reconstruction of the cascade L-C system, as well as offering a straightforward interpretation of its result, since output $K_{m3}(c) = 0$ implies a non-chaotic time series, while an output $K_{m3}(c) = 1$ means that the analyzed time series is chaotic.

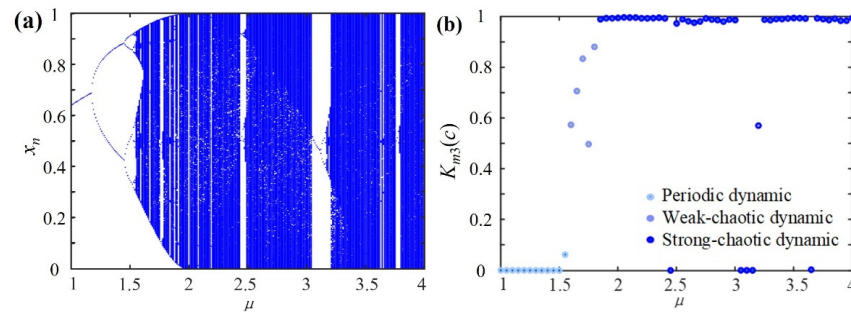


Figure 1. The experimental graphical results of the 0-1 test for chaos when it is used to detect the cascade L-C system (of which the dynamical states are periodic, weak-chaotic, and strong-chaotic) with $1 \leq \mu \leq 4$ increased in increments of $\mu = 0.05$: (a) the bifurcation diagram of the cascade L-C system; (b) the plot of $K_{m3}(c)$ versus μ .

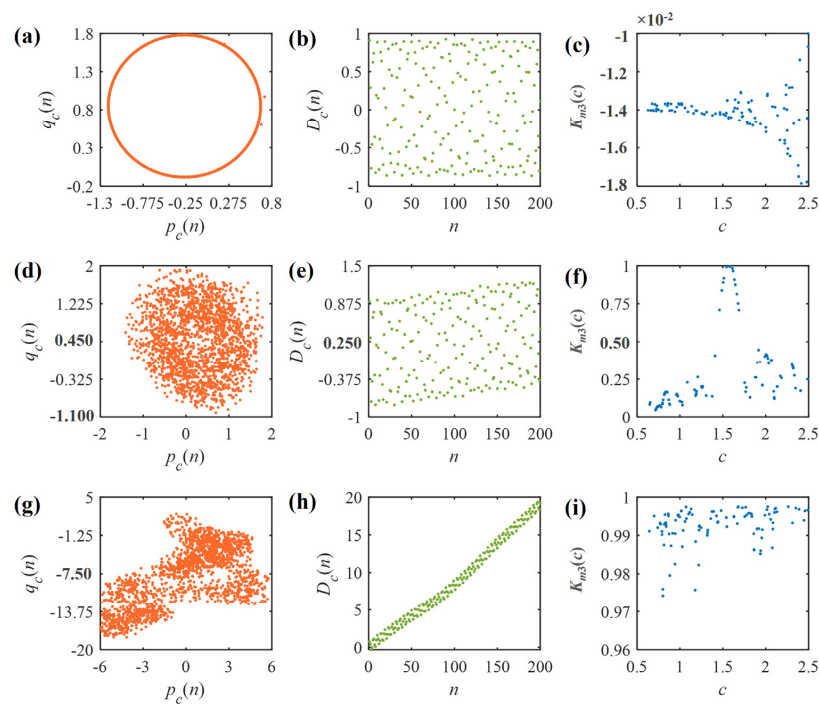


Figure 2. The detection results of the 0-1 test for chaos when it is used to detect the cascade L-C system with different values of μ : from (a–c): $\mu = 1.41$, periodic dynamic; from (d–f): $\mu = 1.56$, weak-chaotic dynamic; from (g–i): $\mu = 3.99$, strong-chaotic dynamic.

3.2. Generation of Noisy Time Series Data

The cascade L-C system with measurement noise is further considered to illustrate the validity of the 0-1 test for chaos. The new data sequence combining the simple noise resulting from the statistical distribution function and the time series resulting from the cascade L-C system is given by

$$\tilde{x}(n) = x(n) \left(1 + \frac{\epsilon}{100} \eta_n \right) \tag{15}$$

where η_n refers to independently and identically distributed random variable drawn from a uniform distribution on $[-1, 1]$ and ϵ is related to the noise-level in percent. In practice, it has been reported from Gottwald and Melbourne (2005) and Schreiber and Kantz (1995) that the amount of contaminated data is limited and for large noise levels the Lyapunov exponents are systematically wrong [29,30]. Since the dataset size has a critical impact on the calculation results, the effect of the sequence size N on the asymptotic growth rate $K_{m4}(c)$ is discussed, as shown in Figure 3. As expected, the diagnostic output $K_{m4}(c)$ is closer to 0 for periodic motion (e.g., the control parameter is $\mu = 1.41$ and the initialization is $x_0 = 0.9$) and 1 for chaotic motion (e.g., the control parameter is $\mu = 3.99$ and the initialization is $x_0 = 0.9$) when the data length is greater than $N = 10^3$. In addition, the same pattern also exists for the different values $\alpha = 2, \alpha = 4, \alpha = 6, \alpha = 8,$ and $\alpha = 10$ of the amplitude parameter. Therefore, it is obvious that the sequence size used in the numerical experiment is related to the results of the 0-1 test for chaos, and the length of the time series used in the numerical investigations is $N = 2.0 \times 10^3$ below.

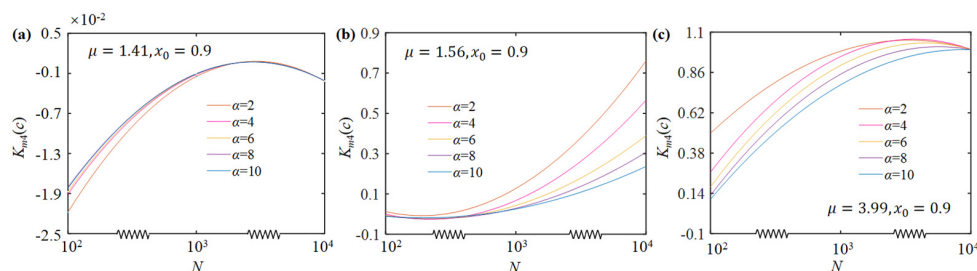


Figure 3. The comparison results of $K_{m4}(c)$ versus N when the modified 0-1 test for chaos is applied to identify the three states. The data length of time series with a noise level of 5% for the cascade L-C system is $N = 2.0 \times 10^3$, the initialization is $x_0 = 0.9$, and the amplitude parameter α is different, as mentioned above: (a) $\mu = 1.41$ corresponds to periodic motion; (b) $\mu = 1.56$ corresponds to weak-chaotic motion; (c) $\mu = 3.99$ corresponds to strong-chaotic motion).

4. Results and Discussion

4.1. Effect of the Frequency ω on $K_{m4}(c)$

In terms of cascade dynamical system, as mentioned above, the chaotic indicator $K_{m4}(c)$ involves two sensitivity parameters: the frequency ω and amplitude α . In this section, the numerical values of $K_{m4}(c)$ for frequency parameter changing from $\omega = 0$ to $\omega = 10$ are provided, as shown in Figure 4. According to this figure, periodic dynamic is represented by the blue line, weak-chaotic dynamic is represented by the purple line, and strong-chaotic dynamic is represented by the red line. As expected, the numerical values of $K_{m4}(c)$ corresponding to the three states own different significant fluctuations due to frequency ω . It should be noted that the strong-chaotic dynamic (see the red line) shows the least range of fluctuation of $K_{m4}(c)$ which is related to ω . Meanwhile, the fluctuation of $K_{m4}(c)$ is increased with the increasing of amplitude from $\alpha = 2$ to $\alpha = 10$, and remains stable at $K_{m4}(c) = 1$ approximately. In addition, the chaotic indicator $K_{m4}(c)$ for the weak-chaotic dynamic (see the purple line) is most sensitive to the changing of the frequency parameter ω . This is because there exists a significant drop of $K_{m4}(c)$ at the beginning, and then the asymptotic growth rate fluctuates around $K_{m4}(c) = 0.35$. Furthermore, it reaches a low point at $\omega = 44$ while the asymptotic growth rate is $K_{m4}(c) = 0.2$. It is also obvious

that the asymptotic growth rate corresponding to the periodic dynamic fluctuates around $K_{m4}(c) = 0$ and more significantly than that corresponding to the strong-chaotic dynamic. Furthermore, the asymptotic growth rate corresponding to the periodic dynamic is very similar to that corresponding to the weak-chaotic dynamic and drops to $K_{m4}(c) = 0.4$ at $\omega = 44$.

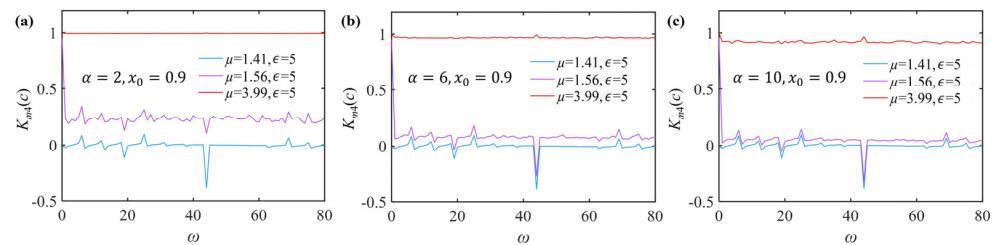


Figure 4. The comparison results of $K_{m4}(c)$ with the changing of ω when the modified 0-1 test for chaos is applied to detect the three states ($\mu = 1.41$ corresponds to periodic motion, $\mu = 1.56$ corresponds to weak-chaotic motion, and $\mu = 3.99$ corresponds to strong-chaotic motion) of the cascade dynamical system. For the cascade L-C system, the data length of time series with a noise level of 5% is $N = 2.0 \times 10^3$, the initialization is $x_0 = 0.9$, and the values of the amplitude parameter are provided differently: (a) $\alpha = 2$; (b) $\alpha = 6$; (c) $\alpha = 10$.

In summary, the changing of the frequency parameter ω owns a small effect on improving the accuracy of the modified 0-1 test for chaos when the cascade dynamical system is investigated. However, the frequency ω of the asymptotic growth rate has different behaviors for regular, weak-chaotic, and strong-chaotic time series of the cascade L-C dynamical system. In other words, the ω effect is provided for the first time to fill the gap in the literature. In addition, for $\alpha = 2$, $\alpha = 6$, and $\alpha = 10$, the asymptotic growth rate $K_{m4}(c)$ corresponding to weak-chaotic sequence seems to be most sensitive to the amplitude parameter α when the modified version of 0-1 test for chaos is used to identify the three deterministic states, as shown in Figure 4. When the $K_{m4}(c)$ values decrease significantly with increasing α values, for the periodic and weak-chaotic sequences, the two minimum values of $K_{m4}(c)$ decrease significantly and are both at the same point with $\omega = 44$. However, whether the changing of amplitude α can significantly affect the status identification of the cascade dynamical system or not is needed to discuss with much narrower step sizes. In particular, the frequency ω is taken as a fixed numerical value $\sqrt{2}$ in the open literature, so the frequency ω is taken as the same fixed numerical value for an in-depth discussion below.

4.2. Effect of the Amplitude α on $K_{m4}(c)$

Figure 5 shows the trend of the asymptotic growth rate $K_{m4}(c)$, with the amplitude parameter changing from $\alpha = 0$ to $\alpha = 10$ when the 0-1 test for chaos is used to identify the status of the noisy cascade dynamical system with different noise-level. According to Figure 5a, the changing trends of the asymptotic growth rate $K_{m4}(c)$ corresponding to the three states, including periodic pattern, weak chaos, and strong chaos, are completely different as the amplitude parameter α increases. From Figure 5b, slight fluctuations of AGRs occur for the periodic dynamic. Specifically, for the AGRs there are significant downward trends when $\alpha \in [0, 0.4]$, slight rises when $\alpha \in [0.4, 1.5]$, and narrow fluctuation around a fixed value which is less than $K_{m4}(c) = 0$ when $\alpha \in [1.5, 10]$. From Figure 5c, sharp declines of AGRs occur for the weak-chaotic dynamic, and for the AGRs there are slight and negligible fluctuations around $K_{m4}(c) = 0$ after the amplitude parameter increases to $\alpha = 5$ to a first approximation. From Figure 5d, slight declines of AGRs occur for the strong-chaotic dynamics and the values of AGR are all greater than $K_{m4}(c) = 0.9$ when $\alpha \in [0, 10]$.

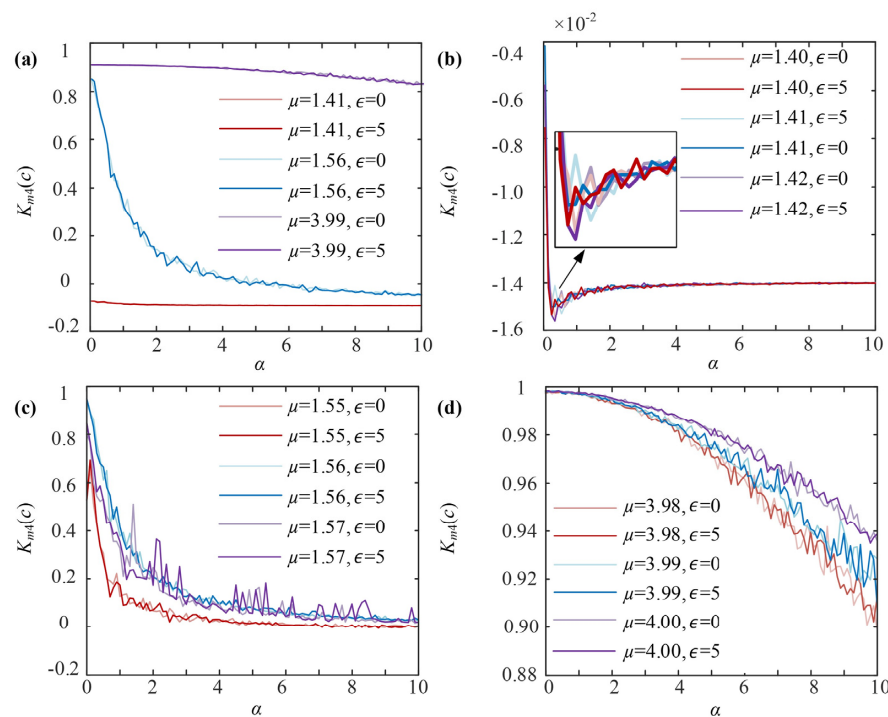


Figure 5. The comparison results of $K_{m4}(c)$ change with α when the modified 0-1 test for chaos is used. The data length of the no-noise or noisy time series from the cascade L-C system is $N = 2.0 \times 10^3$ and the initialization is $x_0 = 0.9$: (a) the comparison results for the three states ($\mu = 1.41$ corresponds to periodic motion, $\mu = 1.56$ corresponds to weak-chaotic motion, and $\mu = 3.99$ corresponds to strong-chaotic motion); (b) the results for periodic time series with different μ values and noise levels ϵ ; (c) the results for weak-chaotic time series with different μ values and noise levels ϵ ; (d) the results of strong-chaotic time series with different μ values and noise levels ϵ .

Table 3 reflects the quantitative data on the decrease of the asymptotic growth rate with respect to the weakly and strongly chaotic dynamics. According to this table, for the weak-chaotic dynamics with $\mu = 1.55$, $\mu = 1.56$, and $\mu = 1.57$ and measurement noise with $\epsilon = 0$ and $\epsilon = 5$, the ratio of difference value (between the initial and final AGRs) and initial AGR shows a decreasing trend from 99% to 97%, approximately. For the strong-chaotic dynamics with $\mu = 3.98$, $\mu = 3.99$, and $\mu = 4.00$, and the added noise with two levels, meanwhile, the ratio represents a descending tendency from 9% to 6%, approximately. In addition, the effects of noise levels (i.e., $\epsilon = 0$ and $\epsilon = 5$) on the ratio are not distinct. In fact, measurement noise refers to the corruption of observations by errors which are independent of the dynamics. The modified 0-1 test for chaos owns good robustness with respect to the measurement noise. It can be obviously concluded that the AGR presents the greater drop for weak-chaotic dynamic (i.e., $K_{m4}(c)$ rapidly approaches 0) than that for strong-chaotic dynamic.

Table 3. Quantitative data on decrease of $K_{m4}(c)$ in terms of weakly and strongly chaotic sequences.

System Status	Control Parameter	Ratio of Difference Value and Initial AGR	
		$\epsilon=0$	$\epsilon=5$
Level of the Added Noise			
Weak-chaotic dynamic	$\mu = 1.55$	99.68%	99.04%
	$\mu = 1.56$	96.54%	96.87%
	$\mu = 1.57$	97.23%	97.14%
Strong-chaotic dynamic	$\mu = 3.98$	8.96%	9.85%
	$\mu = 3.99$	8.49%	7.80%
	$\mu = 4.00$	6.15%	5.91%

For the effect of measurement noise and amplitude parameter, the further discussion for the differentiation of dynamical states is provided below. As shown in Figure 6, the values of $K_{m4}(c)$ corresponding to the three states of the cascade L-C system fluctuate after adding noise from 0 to 100%. It is to be noted that the $K_{m4}(c)$ do not monotonically increase or decrease with the increasing of noise level. As expected, the fluctuation of $K_{m4}(c)$ represents stable with respect to the periodic dynamic, violent with respect to the weak-chaotic dynamic, and slighter with respect to the chaotic dynamic as the noise level increases. It is shown that the modified 0-1 test for chaos is robust for the measurement noise, and the sensitivity parameters can improve the anti-noise performance of the 0-1 test for chaos. This investigation also confirms that there is a very necessary to select appropriate parameter α to significantly improve the best detection performance of the modified 0-1 test for chaos.

For the above investigations related to L-C system, the amplitude parameter α has little influence on the chaos indicator when the 0-1 test for chaos is applied to the periodic sequence. For strongly chaotic sequence, the values of $K_{m4}(c)$ decrease due to the increase of the amplitude parameter α . The effect of amplitude parameter α on the AGR $K_{m4}(c)$ cannot be neglected as well when the modified 0-1 test for chaos is considered in terms of the weakly chaotic sequence. Furthermore, the values of amplitude parameter α that are selected for the modified 0-1 test for chaos can greatly affect the detection output for weak-chaotic systems. The variations of $K_{m4}(c)$ with α hence follow a clear pattern regarding the periodic, weak-chaotic, and strong-chaotic dynamics. Then, the changing of $K_{m4}(c)$ with α can be used as an auxiliary judgment criterion for the 0-1 test for chaos and the added noise does not have a great effect on the changing tendency.

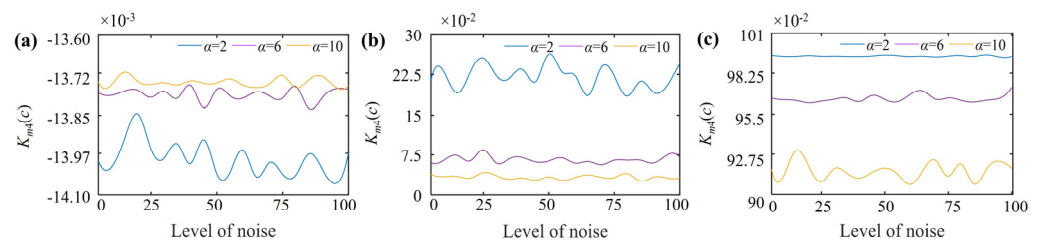


Figure 6. The comparison results of $K_{m4}(c)$ versus level of the added noise the step-length of 5% when the modified 0-1 test for chaos is applied to test three states: (a) the results of periodic dynamic; (b) the results of weak-chaotic dynamic; (c) the results of strong-chaotic dynamic.

4.3. Effect of the Amplitude α on $D_c^*(n)$

When it has been verified that the changing of the asymptotic growth rate $K_{m4}(c)$ with the amplitude parameter α can be used as an auxiliary judging criterion for the 0-1 test for chaos, the next step is to discuss whether the changing of $K_{m4}(c)$ with α can be used as the auxiliary judging criterion for detecting the cascade L-C dynamical system with the three numerical values of control parameter μ . In the previous section, the approach of $D_c^*(n)$ has been given, which is the important parameter for using the modified 0-1 test for chaos. The comparison results of $D_c^*(n)$ with two different values of the amplitude parameter are provided for detecting the synthetical time series with initial value $x_0 = 0.9$, as shown in Figure 7. The six contaminated sequences with the finite data length $N = 2.0 \times 10^3$ and the added uniform noise $\epsilon = 5$ are considered here as the testing time series. In particular, the step size is taken by $\Delta n = 5$ in terms of the data length $N = 2.0 \times 10^3$. In addition, the amplitude parameters of the three sequences corresponding to the red lines are all $\alpha = 1$ while the others corresponding to blue lines are all $\alpha = 10$. According to this figure, the periodic and weak-chaotic cascade sequences exhibit obviously similar nonlinear characteristic, and the values of their fluctuation range $\Delta D_c^*(n)$ are not greater than 8.5. However, the chaos indicator $D_c^*(n)$ corresponding to the strong-chaotic time series greatly increases linearly. It is also shown that there exists a strong sensitivity of amplitude parameter α to the version $D_c^*(n)$ of the modified mean square displacement

$D_c(n)$ and the increased values of α can exacerbate the fluctuation of the $D_c^*(n)$ when the 0-1 test for chaos is used to identify the different status of the cascade dynamic systems.

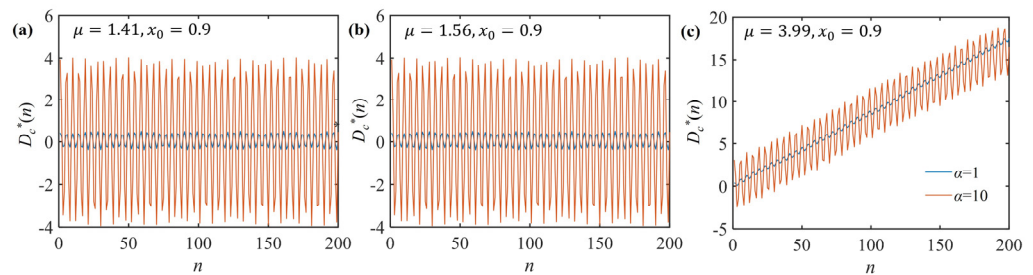


Figure 7. The comparison results of $D_c^*(n)$ with two different values $\alpha = 1$ and $\alpha = 10$ of the amplitude parameter which is related to detect the synthetical time series generated by combining the simple uniform noise and the three cascade L-C mapping: (a) $\mu = 1.41$ corresponds to periodic dynamic, (b) $\mu = 1.56$ corresponds to weak-chaotic dynamic, and (c) $\mu = 3.99$ corresponds to strong-chaotic dynamic.

All things considered, the changing of $D_c^*(n)$ with n can also be used as an auxiliary indicator to evaluate the nonlinearity of the cascade time series and the tendency of values of $D_c^*(n)$ as a function of n is changing quite a bit between $\alpha = 1$ (blue line) and $\alpha = 10$ (red line) for the noisy cascade time series. In weakly chaotic systems, from the open literature, the regions of regular (periodic and quasiperiodic) and chaotic motions typically coexist in the phase space. The amplitude parameter α associated with V_{damp} controls the sensitivity of the test to weak chaos and to noise when the 0-1 test for chaos is used to distinguish between chaotic and nonchaotic behavior in noise-contaminated, essentially stationary, and deterministic time series data. In fact, the asymptotic growth rate is determined by the mean square displacement of which the original and modified version own the same changing pattern. From the previous text, the amplitude parameter α is a key factor which has an impact on $K_{m4}(c)$ when the noisy cascade dynamical system comes down to chaos detection. Considering the change of $D_c^*(n)$ with α , however, it is not easy to provide the obvious difference between the calculations corresponding to the periodic and weak-chaotic time series data. Therefore, the present alternative approach for identifying nonlinear dynamics of the cascade system is far superior to traditional methods without preprocessing the data with standard noise reduction methods.

5. Conclusions

Developing a reliable and proper diagnosis tool is one of most important things to the utilization of cascading chaotic systems. In this work, a simple, convenient test for chaos is investigated and its efficiency is tested with the cascading chaotic systems (i.e., the cascade L-C system) which is a typical nonlinear dynamic system. Then, the effects of the sensitivity parameters, including the frequency parameter ω and the amplitude parameter α on the chaos indicator of the modified 0-1 test for chaos, are discussed by designing numerical experiments. The following is a summary of the present conclusions. (1) The numerical simulation results show that the periodic, weak-chaotic, and strong-chaotic dynamics of the cascade L-C system can be easily distinguished by the 0-1 test for chaos. (2) The changing of the frequency parameter ω has a small effect on the AGR K_m , as for the modified 0-1 test for chaos, while the changing of the amplitude parameter α can significantly affect the AGR K_m . (3) The changing of K_m with α can be used as an auxiliary judgment criterion for testing the cascade chaotic systems, while the changing of $D_c^*(n)$ with n can be used as an additional diagnose criterion to distinguish the weak-chaotic dynamic and strong-chaotic dynamic. From the perspective of chaos detection, hence, the further understanding of nonlinearity of the cascading chaotic system is provided by investigating the sensitivity parameters of the 0-1 test for chaos in this work. In addition, the effect of sensitivity parameters for some

other varieties of measurement noise (i.e., Gaussian noise, Impulsive noise, Rayleigh noise, Gamma noise, or Exponential noise) will be investigated in the future.

Author Contributions: Y.L.: Data curation, investigation, methodology, and writing-original draft preparation. K.Y.: Conceptualization, validation, software. H.W.: writing-review and editing. Q.X.: Conceptualization, project administration, funding acquisition and supervision. All authors have read and agreed to the published version of the manuscript.

Funding: This research was funded by the Natural Science Foundation of Yunnan Province, China (No. 202101AU070031) the Scientific Research Fund Project of Yunnan Education Department, China (No. 2021J0063), and Young Elite Scientist Sponsorship Program by CAST, China (No. YESS20210106).

Institutional Review Board Statement: Not applicable.

Informed Consent Statement: Not applicable.

Data Availability Statement: Not applicable.

Acknowledgments: The authors wish to acknowledge the Editors and anonymous reviewers for their constructive comments and suggestions, which helped us to improve the manuscript. This work was financially supported by the Natural Science Foundation of Yunnan Province, China (No. 202101AU070031) the Scientific Research Fund Project of Yunnan Education Department, China (No. 2021J0063), and Young Elite Scientist Sponsorship Program by CAST, China (No. YESS20210106).

Conflicts of Interest: The authors declare no conflict of interest.

References

1. André, H.E.; Susanne, S. On complex dynamics in a Purkinje and a ventricular cardiac cell model. *Commun. Nonlinear Sci. Numer. Simul.* **2021**, *93*, 1055511.
2. Absos, A.; Harekrishna, D. An eco-epidemic predator-prey model with Allee effect in prey. *Int. J. Bifurc. Chaos* **2020**, *13*, 2050194.
3. Li, M.; Wang, Y.; Geng, J.; Hong, W. Chaos cloud quantum bat hybrid optimization algorithm. *Nonlinear Dyn.* **2021**, *103*, 1167–1193. [[CrossRef](#)]
4. Wang, X.; Zhang, M. An image encryption algorithm based on new chaos and diffusion values of a truth table. *Inf. Sci.* **2021**, *579*, 128–149. [[CrossRef](#)]
5. Blake, M.; Davison, R.A. Chaos and pole-skipping in rotating black holes. *J. High Energy Phys.* **2022**, *2022*, 13. [[CrossRef](#)]
6. Choi, C.; Mezei, M.; Sárosi, G. Pole skipping away from maximal chaos. *J. High Energy Phys.* **2021**, *2021*, 207. [[CrossRef](#)]
7. Bedrossian, J.; Blumenthal, A.; Punshon-Smith, S. Almost-sure enhanced dissipation and uniform-in-diffusivity exponential mixing for advection-diffusion by stochastic Navier-Stokes. *Probab. Theory Relat. Fields* **2021**, *179*, 777–834. [[CrossRef](#)]
8. Gu, D.; Liu, Z.; Li, J.; Xie, Z.; Tao, C.; Wang, Y. Intensification of chaotic mixing in a stirred tank with a punched rigid-flexible impeller and a chaotic motor. *Chem. Eng. Processing Process Intensif.* **2017**, *122*, 1–9. [[CrossRef](#)]
9. Ouannas, A.; Khennaoui, A.A.; Momani, S.; Grassi, G.; Pham, V.T.; Khazali, R.; Vo Hoang, D. A quadratic fractional map without equilibria: Bifurcation, 0-1 test, complexity, entropy, and control. *Electronics* **2020**, *9*, 748. [[CrossRef](#)]
10. Gottwald, G.A.; Melbourne, I. A new test for chaos in deterministic systems. *Proc. R. Soc. Lond. Ser. A Math. Phys. Eng. Sci.* **2004**, *460*, 603–611. [[CrossRef](#)]
11. Rosa, L.A.S.; Prebianca, F.; Hoff, A.; Manchein, C.; Albuquerque, H.A. Characterizing the dynamics of the Watt governor system under harmonic perturbation and Gaussian noise. *Int. J. Bifurc. Chaos* **2020**, *30*, 2030031. [[CrossRef](#)]
12. Srivastava, A.K.; Tiwari, M.; Singh, A. Composite test inclusive of Benford's law, noise reduction and 0-1 test for effective detection of chaos in rotor-stator rub. *Nonlinear Dyn.* **2021**, *106*, 989–1010. [[CrossRef](#)]
13. Toker, D.; Sommer, F.T.; D'Esposito, M. A simple method for detecting chaos in nature. *Commun. Biol.* **2020**, *3*, 11. [[CrossRef](#)] [[PubMed](#)]
14. He, Z.; Abbes, A.; Jahanshahi, H.; Alotaibi, D.N.; Wang, Y. Fractional-order discrete-time SIR epidemic model with vaccination: Chaos and complexity. *Mathematics* **2022**, *10*, 165. [[CrossRef](#)]
15. Wang, L.; Mao, X.; Wang, A.; Wang, Y.; Gao, Z.; Li, S.; Yan, L. Scheme of coherent optical chaos communication. *Opt. Lett.* **2020**, *45*, 4762–4765. [[CrossRef](#)]
16. Abdullah, H.A.; Abdullah, N.H.; Mahmoud Al-Jawher, A.W. A hybrid chaotic map for communication security applications. *Int. J. Commun. Syst.* **2020**, *33*, e4236. [[CrossRef](#)]
17. Gottwald, G.A.; Melbourne, I. On the implementation of the 0-1 test for chaos. *SIAM J. Appl. Dyn. Syst.* **2009**, *8*, 129–145. [[CrossRef](#)]
18. Armand Eyebe Fouda, J.S.; Bertrand, B.; Sabat, S.L.; Yves Effa, J. A modified 0-1 test for chaos detection in oversampled time series observations. *Int. J. Bifurc. Chaos* **2014**, *24*, 1450063–1450064. [[CrossRef](#)]

19. Muthu, J.S.; Paul, A.J.; Murali, P. An efficient analysis of the behavior of one-dimensional chaotic maps using 0-1 test and three state test. In Proceedings of the 2020 IEEE Recent Advances in Intelligent Computational Systems (RAICS), Trivandrum, India, 3–5 December 2020; pp. 125–130.
20. Xiao, Q.; Liao, Y.; Xu, W.; Chen, J.; Wang, H. Impact of damping amplitude on chaos detection reliability of the improved 0-1 test for oversampled and noisy observations. *Nonlinear Dyn.* **2022**, *108*, 4385–4398. [[CrossRef](#)]
21. Chen, Z.; Liang, D.; Deng, X.; Zhang, Y. Performance analysis and improvement of logistic chaotic mapping. *J. Electron. Inf. Technol.* **2016**, *38*, 1547–1551.
22. Zhuang, Z.; Jing, W.; Liu, J.; Yang, D.; Chen, S. A new digital image encryption algorithm based on improved Logistic mapping and Josephus circle. *J. Comput. Commun.* **2018**, *6*, 14–28. [[CrossRef](#)]
23. Guo, Y.; Jing, S.; Zhou, Y.; Xu, X.; Wei, L. An image encryption algorithm based on Logistic-Fibonacci cascade chaos and 3D bit scrambling. *IEEE Access* **2020**, *8*, 9896–9912. [[CrossRef](#)]
24. Cheng, S.; Sun, J.; Xu, C. A color image encryption scheme based on a hybrid cascaded chaotic system. *Int. J. Bifurc. Chaos* **2021**, *31*, 2150125–2150136. [[CrossRef](#)]
25. Jin, J.; Lin, R.; Zhang, Q.; Hou, G.; Di, Z.; Jia, C. Real-time speech audio domain encryption system based on chaotic cascade. *Comput. Eng.* **2009**, *35*, 137–139.
26. Yu, Y.; Wang, Y.; Wang, C. An iterative cascade chaotic spread spectrum sequence and its performance analysis. *Appl. Electron. Tech.* **2016**, *42*, 95–98.
27. Zhao, L.; Bao, L.; Ding, H. ST linear coupling cascade chaotic spread spectrum code and its performance analysis. *Telecommun. Eng.* **2021**, *61*, 218–223.
28. Zhang, L.; Yang, K.; Li, M.; Xiao, Q.; Wang, H. Enhancement of solid-liquid mixing state quality in a stirred tank by cascade chaotic rotating speed of main shaft. *Powder Technol.* **2022**, *397*, 117020–117026. [[CrossRef](#)]
29. Gottwald, G.A.; Melbourne, I. Testing for chaos in deterministic systems with noise. *Phys. D Nonlinear Phenom.* **2005**, *212*, 100–110. [[CrossRef](#)]
30. Schreiber, T.; Kantz, H. Noise in chaotic data: Diagnosis and treatment. *Chaos Interdiscip. J. Nonlinear Sci.* **1995**, *5*, 133–142. [[CrossRef](#)]